The impact of brain lesions on tDCS-induced electric field magnitude

Ainslie Johnstone [1], Catharina Zich [1,2], Carys Evans [1], Jenny Lee [1], Nick Ward [1,3,4], Sven Bestmann [1,5]

Affiliations

1. Department for Clinical and Movement Neuroscience, UCL Queen Square Institute of Neurology, University College London, London, UK
2. Wellcome Centre for Integrative Neuroimaging, FMRIB, Nuffield Department of Clinical Neurosciences, University of Oxford, Oxford, UK
3. The National Hospital for Neurology and Neurosurgery, London, UK
4. UCLP Centre for Neurorehabilitation, London, UK
5. Wellcome Centre for Human Neuroimaging, UCL Queen Square Institute of Neurology, University College London, London, UK

Word Count: main text ~3800 words + 245 word abstract

Highlights

- Lesions can alter tDCS-induced electric field magnitude (e-mag) in a target by 30%
- The effect of a lesion is greatest if it is large and close to the target
- Lesion conductivity - the true value for which is unknown - also impacts the change
- Lesions can cause increases or decreases to e-mag
- Direction of change depends on the position of the lesion relative to current flow

Abstract (241 words)

Background: Transcranial direct current stimulation (tDCS) has been used to enhance motor and language rehabilitation following a stroke. However, improving the effectiveness of clinical tDCS protocols depends on understanding how a lesion may influence tDCS-induced current flow through the brain.

Objective: We systematically investigated the effect of brain lesions on the magnitude of electric fields (e-mag) induced by tDCS.

Methods: We simulated the effect of 630 different lesions - by varying lesion location, distance from the region of interest (ROI), size and conductivity - on tDCS-induced e-mag. We used current flow models in the brains of two participants, for two commonly used tDCS montages, targeting either primary motor cortex (M1) or Broca's area (BA44) as ROIs.

Results: The effect on *absolute* e-mag change was highly dependent on lesion size, conductance and distance from ROI. Larger lesions, with high conductivity, close to the ROI caused e-mag changes of more than 30%. The *sign* of this change was determined by the location of the lesion. Specifically, lesions located in-line with the predominant direction of current flow increased e-mag in the ROI, whereas lesions located in the opposite direction caused a decrease.

Conclusions: These results demonstrate that tDCS-induced electric fields are profoundly influenced by lesion characteristics. This highlights the need for individualised targeting and dose control in stroke. Additionally, the variation in electrical fields caused by assigned conductance of the lesion underlines the need for improved estimates of lesion conductivity for current flow models.

Keywords:

tDCS, current flow modelling, brain lesions, stroke, electric field

Introduction

Transcranial direct current stimulation (tDCS) is proposed as an economical and non-invasive method of enhancing recovery after stroke when paired with behavioural training [1–10]. However, the effects of tDCS vary substantially across individuals [11,12] making adoption into routine clinical practice difficult. Individual differences in brain and skull anatomy lead to large variations in how much current reaches the target brain regions [13,14]. This leads to unacceptable variability in the physiological and behavioural effects of tDCS across individuals [11,12]. Variability is likely to be further exacerbated in stroke patients where lesions may distort current flow [15]. For example, lesion size and location could influence current flow and are unlikely to be identical in any two patients. Moreover, while it is known that lesions have different conductance compared to healthy brain tissue [16] the magnitude of this difference is not known, and it remains unclear how this affects current flow.

The amount of current, and the path it takes through an individual's brain, can be estimated using current flow modelling [17,18]. Here, high-resolution volume conduction models, usually based on individual MRI scans, apply the laws of electromagnetic induction to the complex geometry of the head and brain. These are often finite element models where the head is segmented into different tissue types, each with an assigned conductivity. Current flow models can be used to estimate variability across individuals [14], determine the individual stimulation intensities required to generate equivalent electric fields across participants [13], or even optimise the electrode location to target specific regions [19–21].

These models have been applied to the brains of stoke patients [15,21–23] with some studies finding profound effects of the lesioned tissue on current flow [15,22]. Despite these efforts, the multi-faceted nature of lesion characteristics and the complexities of their influence(s) on current flow remain unknown. Previous studies are based on the results from one or two example lesions. Across patients, lesions tend to be confined to certain vascular territories but there is large variation in lesion characteristics within these regions, and in principle all areas of the brain have the potential to be affected [24]. Additionally, large variations in stroke size and location can produce similar symptoms [25,26], meaning study or treatment groups are unlikely to have homogenous lesions. This makes it difficult to generalise the conclusions of these previous modelling studies and make decisions on how to incorporate these findings into protocols for individual patients with potentially very different lesions.

A further issue is that the validity of results from current flow modelling simulations rely on the accuracy of tissue segmentation and choice of correct conductance values. Previous studies have opted to model lesions with conductance equivalent to cerebral spinal fluid (CSF) [15,21–23] but the actual conductance value of this tissue is not known. Estimates obtained from various MRI techniques vary 10-fold [16], ranging from values below that of typical grey and white matter conductance, to above the value typical

assigned to CSF. The influence that changes in lesion conductance have on current flow simulations remains unclear.

In this study, we systematically assessed the influence of synthetic lesions on induced electric field magnitude within two regions of interest: M1 and BA44. By using artificial lesions we could independently vary their location, distance, size and conductance and determine general patterns or rules that govern how lesions might alter current flow. Such knowledge can guide optimisation of montages across different study populations and future research into current flow modelling in stroke.

Methods

Overview

A variety of synthetic spherical lesions were modelled in the brains of two example participants, for two different electrode montages. For each montage a region of interest was defined- motor cortex (M1) and Broca's area (BA44)- and lesions differed in their cardinal direction from the ROI, distance from ROI and size. For each lesion, simulations were run using a range of conductance values.

Participants

The T1-weighted 3D structural MR scans of two healthy females were used in this analysis, both of whom gave informed consent to have their scans used for this purpose. The project was approved by the UCL Research Ethics Committee (project no: 14233/001). P01 was 26 years old at time of scanning, P02 was 25 years old. Both scans took place at the Wellcome Centre for Human Neuroimaging at UCL (WCHN, UCL) on a Siemens 3 Tesla TIM Trio scanner with 64-channel head coil (176 sagittal slices, matrix size 256 x 256, 1mm isotropic resolution, TR/TE=1900/3.96).

Current flow modelling

Current flow modelling was performed using a custom version of ROAST 2.7 [27]. ROAST is a fully automated, open-source MATLAB application that performs segmentation of the brain image (via SPM), places virtual electrodes, performs volumetric meshing (via Iso2Mesh- Fang & Boas, 2009) and solves the finite element model numerically to estimate current flow. By default, ROAST segments the image into 6 tissue types (skin, bone, CSF, grey matter, white matter and air). We modified ROAST (i.e. ROAST-lesion) to incorporate a seventh tissue type (lesion). Consequently, volumetric meshing and solving the finite element model was performed using the 7-tissue head model. With the exception of the additional lesion and the tDCS montage information ROAST 2.7 default settings were used for all simulations. Code for ROAST-lesion is available at [*code provided upon acceptance*].

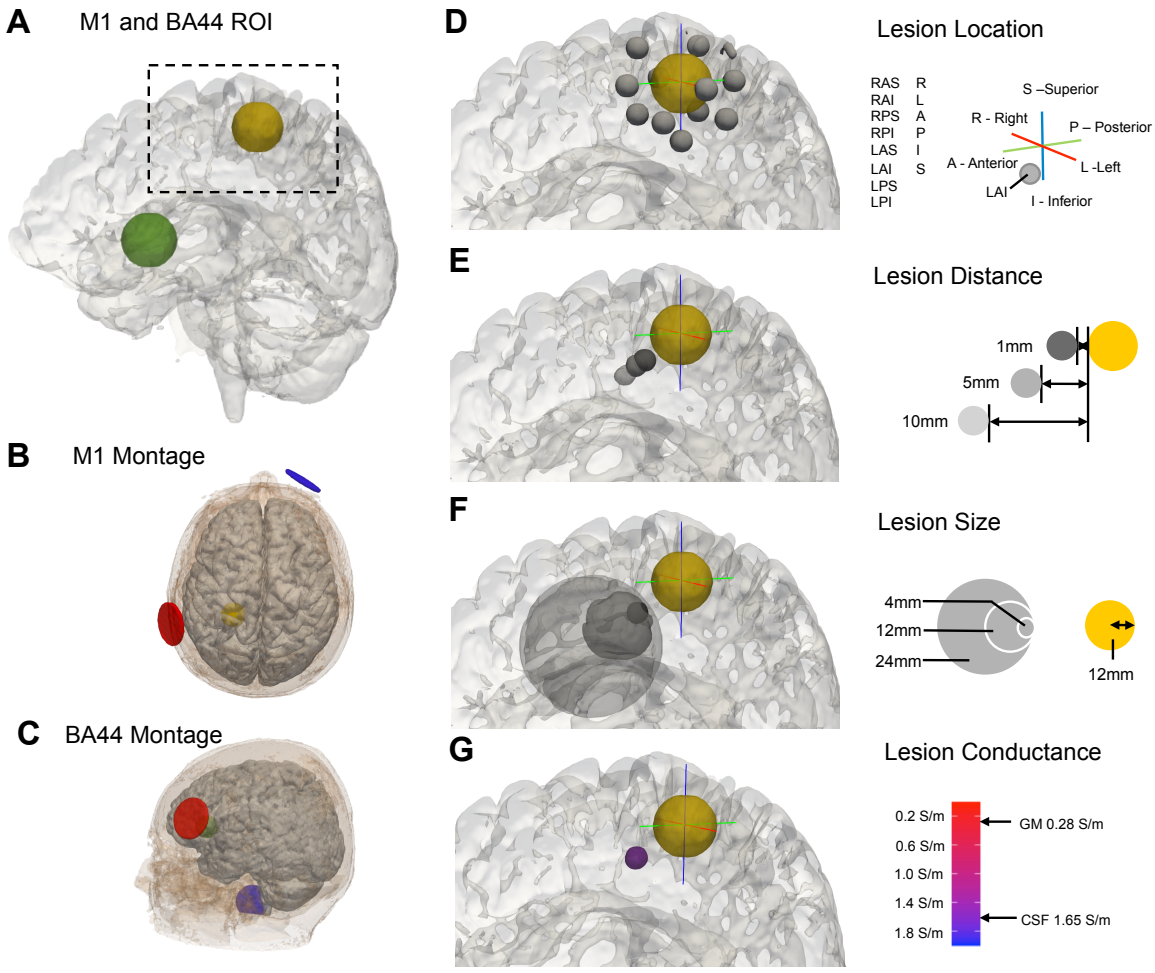

Figure 1: Modelled lesion parameters
A: Rendered brain of example participant (P01) with M1 ROI (yellow) and BA44 ROI (green).
B: tDCS montage targeting M1, with anode in red, cathode in blue.
C: BA44 tDCS montage.
D: The 14 potential lesion directions N.B. lesions where the central voxel was outside the brain were omitted.
E: The three different lesion distances (1mm, 5mm, 10mm), where distance was measured as the shortest Euclidean distance from the edge of the ROI to the edge of the lesion.
F: The three different lesion sizes, defined by lesion radius (4mm, 12mm, 24mm).
G: The five different lesion conductivities (0.2S/m, 0.6S/m, 1S/m, 1.4S/m, 1.8S/m)

tDCS stimulation montages

Two montages with utility in stroke rehabilitation research were selected for this study. One typically used in motor rehabilitation research [29,30] to target M1, where the anode is applied over left primary motor cortex (M1) and the cathode over right supraorbital ridge. Specifically, we placed electrodes over 10-05 coordinates Fp2 and CCP3 for both participants. For the other montage, often used in aphasia rehabilitation studies [7,8] to target BA44, the anode is positioned over left frontal cortex (BA44) and the cathode on the right neck. Specifically, we placed the electrodes over Exx20 and FFT7h for participant one (P01) and over Exx20 and F7h for participant two (P02).

The choice of locations used here are intended to be taken as examples of potential montages. In reality, for many tDCS studies the exact locations of stimulation are individualised either to target intact tissue or to target anatomically or functionally defined regions [31,32]. All simulations were run with an applied current strength of 1mA. It should be noted that, in line with Ohm's Law, e-mag values will scale linearly with increases in applied current given constant conductance. All simulations used disk electrodes of radius 17mm and depth 2mm.

Lesions

Synthetic lesions were positioned relative to the regions of interest (ROI). ROIs were 12mm radius spheres centred at manually defined M1 hand knob, or BA44. All lesions were spherical and constrained to the grey and white matter. The lesions were positioned relative to their cardinal direction from the ROI; either due right (R), left (L), anterior (A), posterior (P), superior (S), inferior (I), right-anterior-superior (RAS), right-anterior-inferior (RAI), right-posterior-superior (RPS), right-posterior-inferior (RPI), left-anterior-superior (LAS), left-anterior-inferior (LAI), left-posterior-superior (LPS), or left-posterior-inferior (LPI) of the ROI (see Figure 1). Lesions varied in distance from the ROIs (shortest Euclidean distance from edge of ROI to edge of lesion: 1mm, 5mm, 10mm), and in size (radii: 4mm, 12mm, 24mm). Lesions were not designed to be morphologically or anatomically realistic, but rather to ensure comparability and quantification of the impact on electrical fields.

Current flow simulations were only performed if the centre of the lesion was within the brain, and if the volume of the lesion was at least 20% of the maximum potential volume. If these conditions were met, then simulations were run with a variety of different lesion conductivities (0.2 S/m, 0.6 S/m, 1 S/m, 1.4 S/m, 1.8 S/m) which ranged from roughly the conductance of grey and white matter (0.28 S/m and 0.13 S/m respectively) to above that of CSF (1.65 S/m), spanning the range of values reported in McCann et al., 2019. Out of a possible 630 simulations, a total of 490 and 409 M1 simulations, and 435 and 355 BA44 were run for P01 and P02 respectfully. Note that there are fewer simulations for the BA44 montage due to the close proximity of the lesion to the cortical surface.

Simulation outputs and independent variables

Electric field magnitude (e-mag) images, measured in V/m, were extracted for each lesion simulation. Additionally, for each participant, and each montage, a simulation without lesions was performed to obtain estimates of e-mag within the 'healthy' non-lesioned brain. The e-mag change for each lesion was calculated by subtracting the non-lesioned e-mag image from the lesioned e-mag image. The mean e-mag change from within the grey matter (GM) of the target ROI was calculated, as well as the 16^{th} and 84^{th} percentile values from within these voxels (see Figure 2)

From the non-lesioned simulation, for each participant, and each montage, the electric field in each direction (R-L, A-P, S-I) for all voxels across the brain was also extracted. The electric field direction vector was calculated, in each participant, for each montage, using the mean electric field in each direction from all the grey matter voxels within the target ROI.

Lesion distance, size and conductivity were treated as continuous numerical variables in all analyses. In order to quantify lesion location and allow for comparison between montages, the angle between the 3D direction vector indicating the movement from the ROI to the lesion, and the 3D electric field direction vector from within the GM of the ROI in the non-lesioned simulation was calculated (see Figure 2E). This created a measure of the degree to which the lesion was located in the path of current flow.

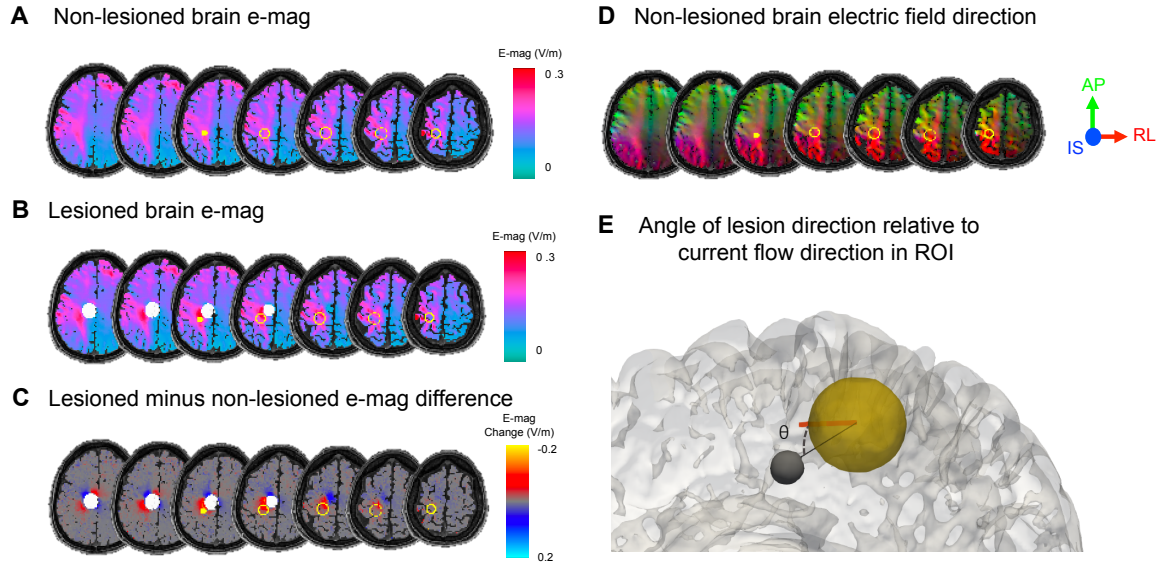

Figure 2: Current flow modelling
A: Electric field magnitude (e-mag) image for M1 montage for the non-lesioned 'healthy' brain of a single subject. M1 outlined in yellow.
B: E-mag image for same montage but in a lesioned brain (filled white circle; RAI lesion, distance 1mm, size 12mm, conductivity 1.2S/m).
C: Difference image (lesioned minus non-lesioned brain). Note the strong increases and decreases around the lesion, reaching magnitudes of approximately +/-0.1V/m.
D: Electric field direction across the brain, coloured by predominant direction of current flow.
E: Calculation of angle between the lesion direction (black line) and the average direction of electric field within the grey matter of the ROI (orange line).

Analysis

All MRI manipulations were performed using tools from the FMRIB software library (FSL; Jenkinson et al., 2012) and all data analysis was performed using R v4.0.3 in RStudio v1.3.1093.

Results

Larger lesions, closer to the ROI, with higher conductivity have a greater impact on e-mag change within ROIs

First, we evaluated the effects of lesion distance, size and conductivity on the *absolute* mean e-mag of the ROI. To this end we used two linear mixed effect models, one for the M1 montage and one for the BA44 montage, with participant as a random effect impacting intercept. For both montages, lesions with closer distance (M1: $F(1,894)=16.9$, $\beta=-0.99$, $p=4.3e-5$, Figure 3A; BA44: $F(1,785)=46.6$, $\beta=-1.05$, $p=2.1e-11$, Figure 3D), larger size (M1: $F(1,894)=90.4$, $\beta=2.31$, $p<2.2e-16$, Figure 3B; BA44: $F(1,785)=178$, $\beta=2.11$, $p<2.2e-16$, Figure 3E), and higher conductance (M1: $F(1,894)=27.4$, $\beta=2.25$, $p=1.4e-10$, Figure 3C; BA44: $F(1,785)=54.6$, $\beta=1.63$, $p=3.8e-13$, Figure 3F) had a greater impact on absolute change in e-mag within the ROI.

There was no change in the significance of results if data from both montages/ROIs were included together in one linear mixed model with montage included as an additional random effect. Adding montage as a fixed effect also did not change results, and there were no significant interactions between montage and the other variables ($p>0.14$) indicating that there was not a significant difference in the effect of lesion distance, size or conductivity on e-mag change between the M1 and BA44 simulations.

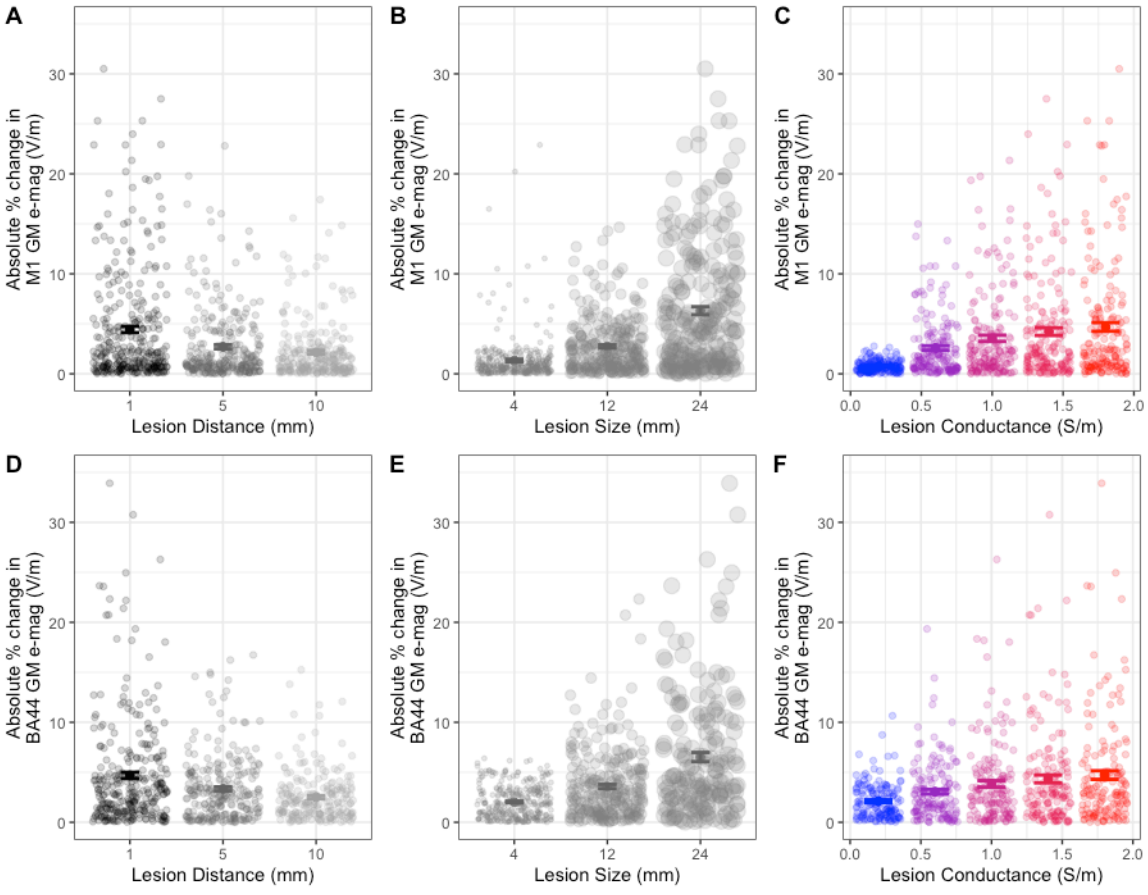

Figure 3: Larger lesions, closer to the ROI, with high conductivity have a greater impact on electric field magnitude (e-mag) change within the ROI

A-C: Scatter plots with mean and standard error (SE) of the *absolute* percentage e-mag changes in M1 caused by lesions with different sizes, distances and conductance. Data are the results from individual simulations and pooled from both participants for analysis.

D-F: Scatter plots with mean and SE of *absolute* e-mag change in BA44 GM.

Individual data points are jittered on the x-axis for display purposes.

Lesions in the path of current flow increase e-mag, while those in the opposite direction cause e-mag decreases

We went on to investigate the main effect of lesion location on the mean e-mag in ROI. Lesions due R, RAS and RAI of left M1 caused increases in M1 e-mag, whereas lesions due inferior, LPI, LAI or RPI tended to decrease M1 e-mag (see Figure 4 for selected examples, and Supplementary Figure 1 for data from all M1 simulations). For the BA44 montage however, lesions due R and RPI tended to increase e-mag within the ROI, whereas lesions due posterior and RAS tended to decrease e-mag (see Supplementary Figure 2 for data from all BA44 simulations).

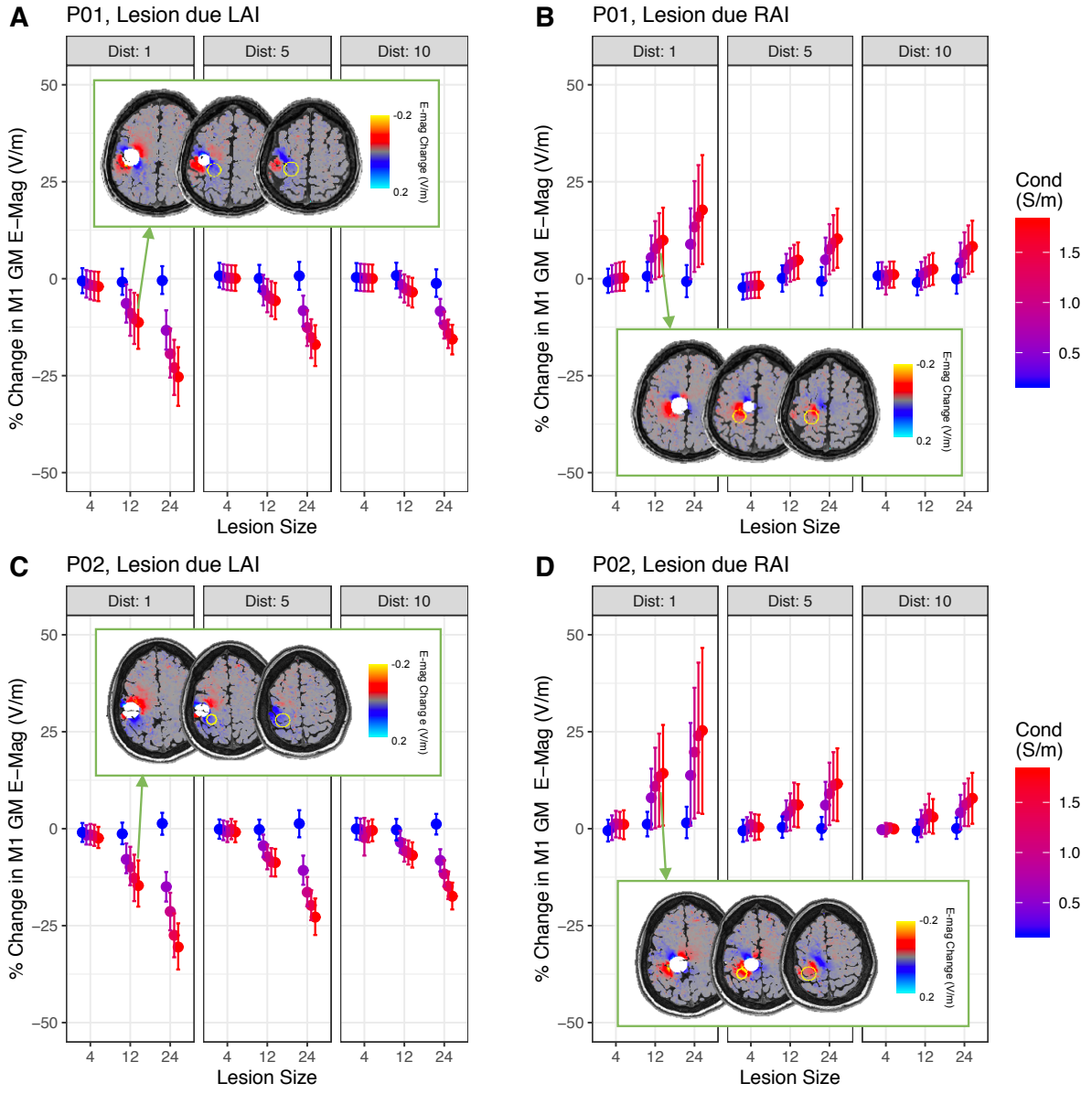

Figure 4: Lesion location determined the sign of electric field magnitude (e-mag) change

A, B: Percentage change in e-mag in M1 region of interest (ROI) caused by lesions due left-anterior-inferior (LAI) or right-anterior-inferior (RAI), with varying distances, sizes and conductivities for participant P01. Data points show mean percentage change across all ROI voxels, error bars show the 16th and 84th percentile values for change across voxels. Inset: Absolute change in e-mag across the whole brain for LAI and RAI lesions of size 12mm, distance 1mm and conductance 1.4S/m.

C,D: Same as above, but for participant P02.

In order to quantify lesion location, and allow comparison between the two montages, the angle of lesion direction relative to the current flow in the ROI was calculated. This was performed by taking the 3D vector linking the centre of the ROI with the centre of the lesion, and the 3D vector describing the electric field direction within the ROI in the non-lesioned brain, and calculating the angle between the two. Angle of lesion location was a significant predictor of percentage change in e-mag in the M1 GM, as assessed by linear mixed model ($t(897)=-9.31$, $\beta=-0.06$, $<2.2e-16$), with participant as a random effect on intercept. The same relationship was found for the BA44 montage ($t(788)=-13.3$, $\beta=-0.07$, $p<2.2e-16$). This indicates that lesions that are more aligned with the direction of current flow in the ROI tended to increase mean e-mag in the ROI, whereas those that were in the opposite direction tended to decrease e-mag.

Combining together data from both montages, with montage as a random effect on intercept, did not change the significance of the effect of lesion location. Including montage as a fixed effect also did not result in a significant main effect of montage, or significant interaction between montage and lesion angle ($p>0.13$), again indicating that the results are consistent across the M1 and BA44 simulations.

Interactions with lesion location

In order to assess whether the effect of lesion location was modulated by the other lesion characteristics, we ran linear mixed models. These included fixed effects of angle of lesion location relative to current flow direction in the ROI, distance, size and conductivity, as well as interactions between angle of lesion location and the other variables. Participant was again included as a random effect on intercepts.

In conformity with the results outlined above, all main effects were significant. Further significant interactions between lesion location and distance (M1: $t(891)=5.27$, $\beta=0.04$, $p=1.7e-7$; BA44: $t(782)=6.83$, $\beta=0.04$, $p=1.7e-11$), lesion location and size (M1: $t(891)=-12.7$, $\beta=-0.09$, $p<2.2e-16$; BA44: $t(782)=-13.0$, $\beta=-0.11$, $p<2.2e-16$), and lesion direction and conductance (M1: $t(891)=-6.02$, $\beta=-0.06$, $p=2.6e-9$; BA44: $t(782)=-9.53$, $\beta=-0.08$, $p<2.2e-16$) were however found. This indicates that lesion direction had a greater effect for lesions with larger size, smaller distance from the ROI and higher conductance (see Figures 5 & 6).

Including all the data, from both montages in a single analysis, with montage as a random effect on slope again did not influence the significance of the results. Furthermore, including montage as a fixed effect resulted in no significant main effect of montage and no significant interactions between montage and any of the other effects or 2-way interactions ($p>0.25$). Once again, this indicates that all effects are consistent across both M1 and BA44 simulations.

247

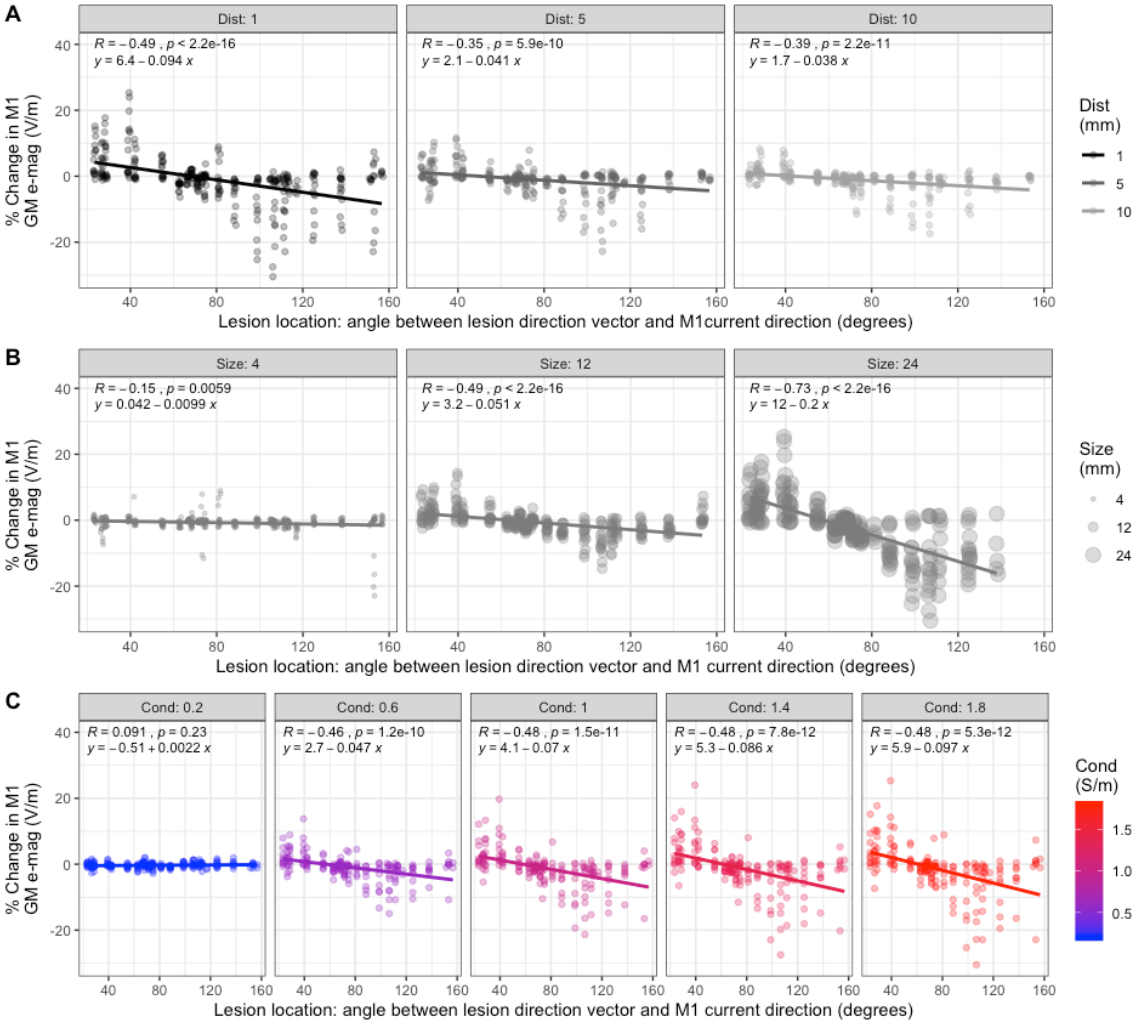

248

Figure 5: Interaction between the effect of lesion location with distance, size and conductance on change in electric field magnitude (e-mag) in M1

A: Changes in e-mag in M1 grey matter (GM) plotted against lesion location, split by lesion distance (in mm). Data from both participants are displayed, and pooled together for analysis. Lesions located in-line with the predominant orientation of current flow in M1 increased e-mag, whereas those in the opposite direction caused a decrease. This was modulated by lesion distance, where closer lesions to the ROI had a greater impact on e-mag change.

B: Changes in e-mag in M1 GM plotted against lesion location, split by lesion size (radius in mm), demonstrating that larger lesions have a greater impact on e-mag change.

C: Changes in e-mag plotted against lesion location, split by conductance (in S/m), showing that lesions with higher conductance have a greater effect on e-mag changes.

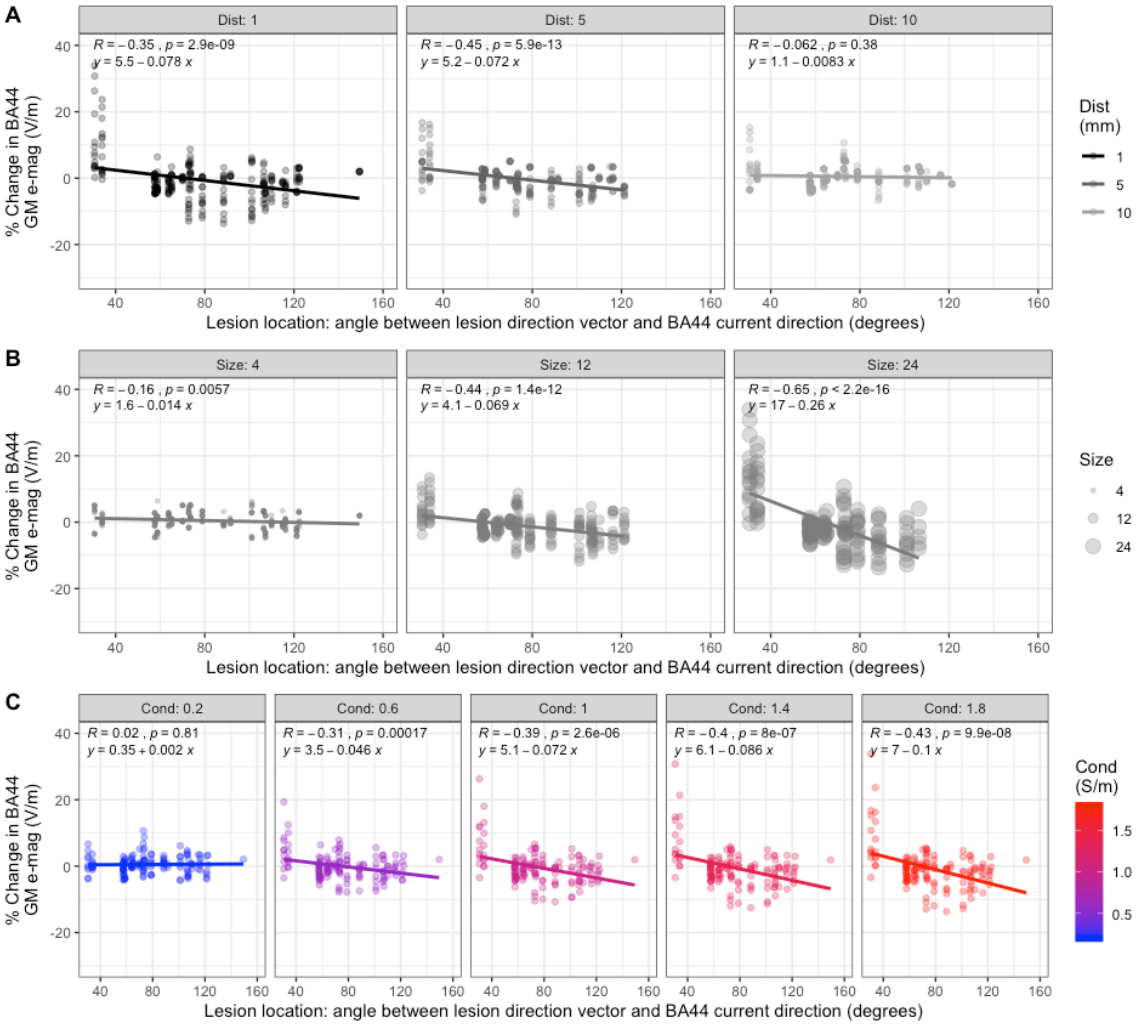

249

Figure 6: Interaction between the effect of lesion location with distance, size and conductance on change in electric field magnitude (e-mag) in BA44

A: Changes in e-mag in BA44 grey matter (GM) plotted against lesion location, split by lesion distance (in mm). Data from both participants are displayed, and pooled together for analysis. Lesions located in-line with the predominant orientation of current flow in BA44 increased e-mag, whereas those in the opposite direction caused a decrease. This was modulated by lesion distance, where closer lesions to the ROI had a greater impact on e-mag change.

B: Changes in e-mag in BA44 GM plotted against lesion location, split by lesion size (radius in mm), demonstrating that larger lesions have a greater impact on e-mag change.

C: Changes in e-mag plotted against lesion location, split by conductance (in S/m), showing that lesions with higher conductance have a greater effect on e-mag changes.

250 # Discussion

251 In this study we modelled the effect of synthetic lesions on tDCS-induced electric field magnitude. We
252 found that distance from the ROI, size and conductance of the lesions all impacted the absolute change in
253 electric field magnitude, with increases or decreases of more than 30%. To further probe why some lesions
254 caused increases in e-mag and others decreases, we investigated the effect of lesion location. We found a
255 systematic effect of location, whereby lesions positioned in-line with the predominant orientation of

current flow in the ROI, where the ROI was located in between the anode and the lesion, tended to increase the magnitude of current flow within that ROI. Lesions that were positioned maximally out-of-line with the current flow caused a decrease in the magnitude of current flow within the ROI. This effect was modulated by the lesion distance, size and conductance. Lesions that were larger, closer to the ROI, and had a higher conductance tended to have the greatest impact - whether positive or negative - on current flow. These effects were consistent when examining both a montage targeting M1, and a montage targeting BA44. Additionally, the same pattern of results was seen in both participant's brains (see Supplementary Figures 1 and 2). Taken together, these results point towards a generalisable pattern in the influence of lesions on tDCS-induced e-mag within ROIs which could be used to guide future studies.

The results presented here build on the findings of previous modelling studies examining the effect of lesions on tDCS-induced current flow patterns [15,21–23]. These studies used MRI scans of real stroke patients, and tended to find that lesions caused a decrease in current flow in the region of interest [15]. Here we show that lesion location, with respect to the direction of current flow, is a key driver in determining the influence of the lesion on current flow, and lesions can cause increases in electric field magnitude in ROIs, as well as decreases.

By modelling synthetic lesions in healthy brains we were able to independently manipulate several lesion parameters to determine their influence on current flow relative to the 'healthy' non-lesioned condition and to each other. This enabled control for inter-individual anatomy, which itself affects current flow, and enabled the use of a wide variety of lesion characteristics which could only be found using a very high number of real patient scans.

Implications for clinical applications

A major issue facing the adoption of brain stimulation techniques into clinical practice is the large inter-individual variability in responses. This variability is likely to be driven, at least in part, by differences in current flow through the regions of interest [34]. In addition to the high degree of variability seen across healthy individuals [13,14], here we show that large lesions will further increase this variability by up to 30%. In the present case, the synthetic nature of our lesions allowed for systematic manipulation of lesion characteristics, but the variability observed here is likely to be amplified in stroke populations with their inherently variable lesion characteristics. Using current flow models to individualise tDCS protocols has been suggested as a method to counter this variability [35] either by altering the intensity of stimulation [13] or by altering electrode placement [19].

The results presented here confirm the need to optimise protocols in order to reduce variability in electric field magnitude. Our results suggest that the distortions in current flow/electrical fields are largest in the

brains of patients with large lesions that are close to the region of interest, and as such the heterogeneity of lesions across patients will amplify the differences in which brain regions are targeted. While simple and freely available methods exist for performing this optimisation [13,21,27] they all rely on having a high resolution whole head MRI of each patient. Obtaining these scans is possible for small well-funded research projects but may not be feasible for large-scale clinical practice given the cost of high-field MRI. The results presented here could be used, in combination with a 2D MR image, to give some indication of whether a lesion is likely to impact the electric field magnitude in a region of interest over-and-above the normal inter-individual variability. Lesions that are small, distant or lie orthogonal to the path of current flow will have little impact on the electric field magnitude within the region of interest.

Important directions for future research

Our results also highlight the effect of assumptions about the lesion conductance on the degree of electric field change caused by a lesion. In order for current flow simulations to provide accurate estimations of electric field magnitude it is essential that appropriate conductance values be assigned to lesions. Previous work has modelled lesions as CSF, which is assigned a very high conductance [15,21–23]. In reality, lesions are not filled with pure CSF and the real conductance is therefore likely to be lower. To the authors knowledge, only one study has investigated the conductance of lesioned tissue using magnetic resonance electrical impedance tomography (MREIT) in a single patient. Here the predicted conductance value was 1.2 S/m in the lesioned tissue [36]. While further research is needed to generate a robust measurement, this value is well below the 1.65 S/m typically assigned to CSF. Our results indicate that lesions with lower conductivity values have less effect on change in e-mag, but conductivities in the region of 1.2 S/m can still result in changes of 20-25%.

In addition to the outstanding question of the conductance of lesioned tissue, segmentation can also be challenging as often lesions do not have clearly defined boundaries. In reality the area typically segmented as a lesion is not homogenous tissue, but rather has a gradient from maximally damaged pure lesioned tissue, through partially affected perilesional tissue, to healthy brain [37]. Rather than having a constant conductance, it is likely that conductance varies across the lesion. Furthermore, conductance may not be stable across time following the stroke; diffusion MRI metrics, which are known to correlate with conductivity [38,39], have been shown to change in the perilesional tissue from acute to chronic stages following stroke [40,41]. In order to ascertain the true effect of lesions on tDCS-induced current flow further work is needed to identify accurate conductivity measures for accurately segmented lesioned tissue and determine whether these values change across time and distance from the lesion centre.

Conclusions

In this study we systematically modelled the influence of synthetic lesions with different locations, sizes and conductivities on the tDCS-induced electric field within two ROIs, for two individuals. Across both ROIs and individuals a general pattern emerged whereby lesions that were lying in-line with the predominant direction of current flow within the non-lesioned brain tended to increase the electric field magnitude in the ROI, while those that were in the opposite direction tended to decrease the electric field in the ROI. This effect was significantly modulated by lesion distance, size and conductance; lesions that were closer to the ROI, larger and had high conductance resulted in the greatest e-mag changes, with increases/decreases of up to 30%. These results demonstrate the potential for increased variability in current flow in the brains of patients, which could in turn impact the behavioural effects of tDCS. We also show that small lesions, far from the region of interest, have relatively little impact on electric field magnitude in the ROI. Finally, our results underline the need for improved estimates of conductivity in lesioned tissue if we are to accurately estimate the true path of current flow through the brains of patients and optimise tDCS for clinical practice.

Acknowledgements

A Johnstone is funded by the Dunhill Medical Trust [RPGF1810\93]; C Zich [201718-13], C Evans and J Lee [201617-03] are funded by Brain Research UK.

Supplementary Figures

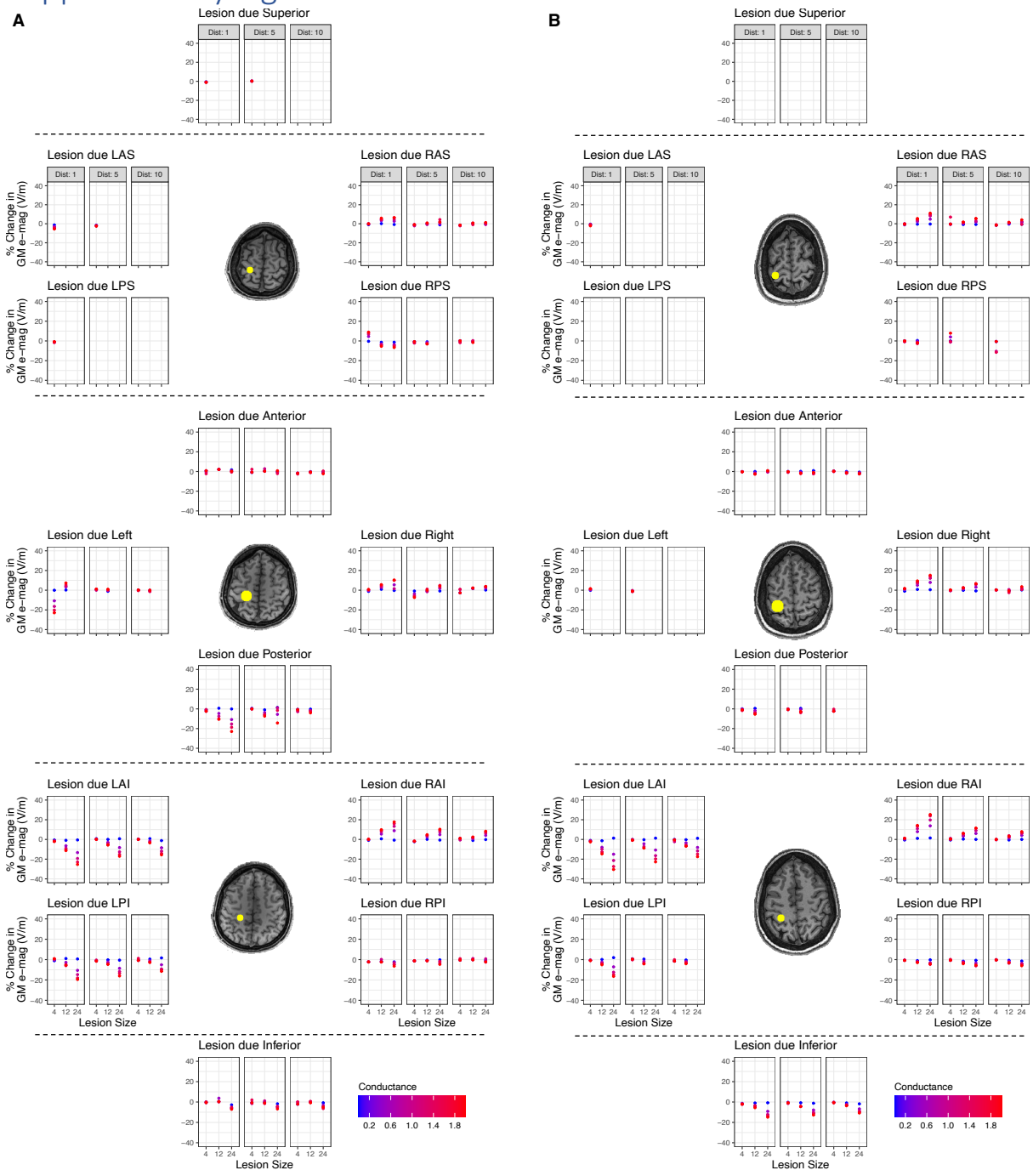

Supplementary Figure 1: Percentage change in M1 electric field magnitude (e-mag) for all lesions

A: Percentage change in e-mag for all lesion locations, sizes (in mm), distances (in mm), and conductivities (in S/m) for participant P01.

B: Same for participant P02

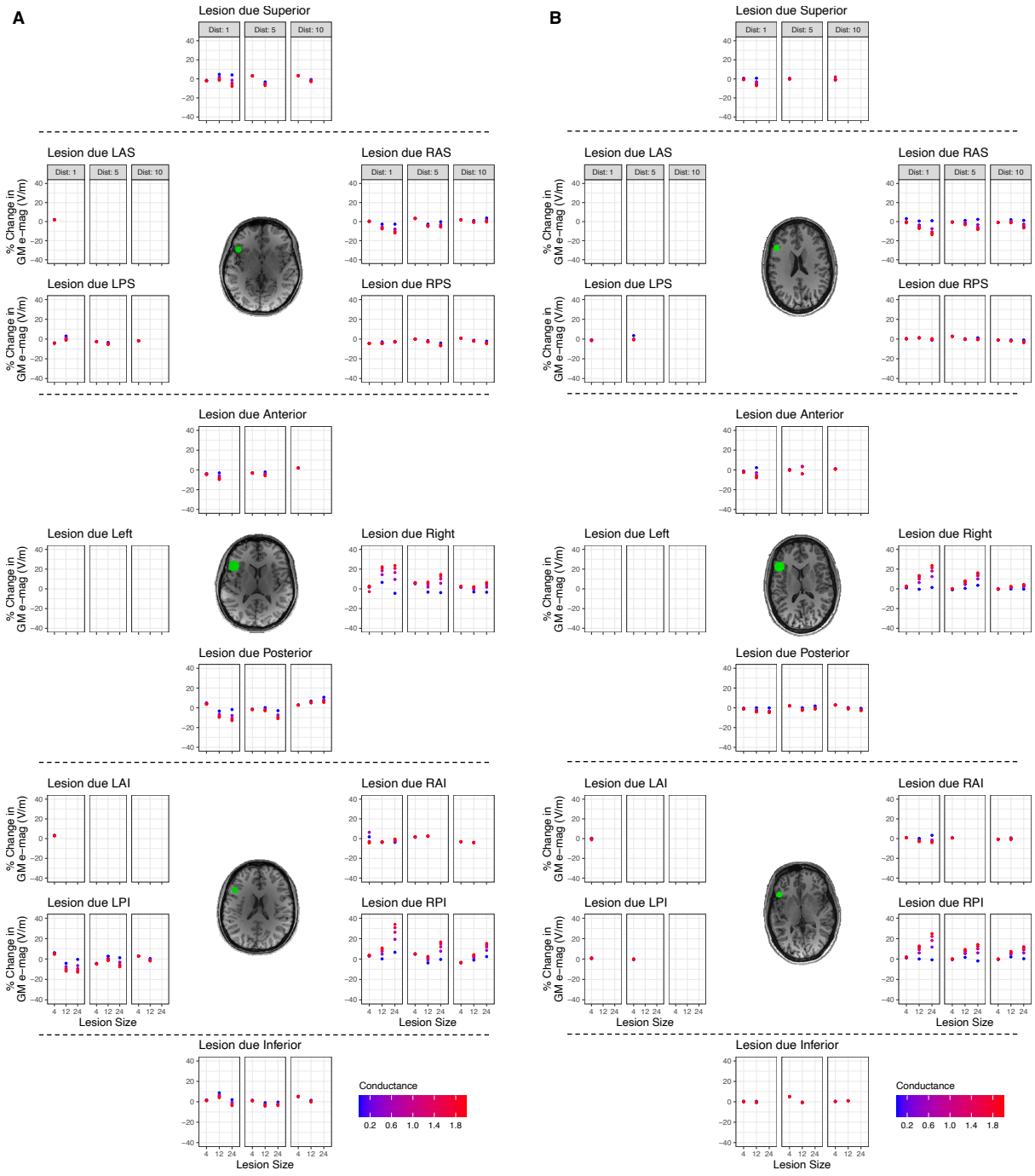

350

351

Supplementary Figure 2: Percentage change in BA44 electric field magnitude (e-mag) for all lesions
A: Percentage change in e-mag for all lesion locations, sizes (in mm), distances (in mm), and conductivities (in S/m) for participant P01.
B: Same for participant P02

352

Bibliography

[1] Kang N, Summers JJ, Cauraugh JH. Transcranial direct current stimulation facilitates motor learning post-stroke: a systematic review and meta-analysis. J Neurol Neurosurg Psychiatry 2015:jnnp-2015.

[2] Stagg CJ, Bachtiar V, O'Shea J, Allman C, Bosnell RA, Kischka U, et al. Cortical activation changes underlying stimulation-induced behavioural gains in chronic stroke. Brain 2012;135:276. https://doi.org/10.1093/brain/awr313.

[3] Hummel F, Celnik P, Giraux P, Floel A, Wu WH, Gerloff C, et al. Effects of non-invasive cortical stimulation on skilled motor function in chronic stroke. Brain 2005;128. https://doi.org/10.1093/brain/awh369.

[4] Hummel FC, Voller B, Celnik P, Floel A, Giraux P, Gerloff C, et al. Effects of brain polarization on reaction times and pinch force in chronic stroke. BMC Neurosci 2006;7:1–10. https://doi.org/10.1186/1471-2202-7-73.

[5] Butler AJ, Shuster M, O'Hara E, Hurley K, Middlebrooks D, Guilkey K. A meta-analysis of the efficacy of anodal transcranial direct current stimulation for upper limb motor recovery in stroke survivors. J Hand Ther 2013;26:162–71. https://doi.org/10.1016/j.jht.2012.07.002.

[6] Allman C, Amadi U, Winkler AM, Wilkins L, Filippini N, Kischka U, et al. Ipsilesional anodal tDCS enhances the functional benefits of rehabilitation in patients after stroke. Sci Transl Med 2016;8:330re1. https://doi.org/10.1126/scitranslmed.aad5651.

[7] Galletta, Conner P, Vogel A, Marangolo P. Use of tDCS in Aphasia Rehabilitation: A Systematic Review of the Behavioral Interventions Implemented With Noninvasive Brain Stimulation for Language Recovery. Am J Speech-Language Pathol 2016;25:S854–67. https://doi.org/10.1044/2016_AJSLP-15-0133.

[8] Holland R, Crinion J. Can tDCS enhance treatment of aphasia after stroke? Aphasiology 2012;26:1169–91. https://doi.org/10.1080/02687038.2011.616925.

[9] Holland R, Leff AP, Josephs O, Galea JM, Desikan M, Price CJ, et al. Speech facilitation by left inferior frontal cortex stimulation. Curr Biol 2011;21:1403–7.

[10] Johnstone A, Levenstein JM, Hinson EL, Stagg CJ. Neurochemical changes underpinning the development of adjunct therapies in recovery after stroke: A role for GABA? J Cereb Blood Flow Metab 2017:0271678X17727670. https://doi.org/10.1177/0271678X17727670.

[11] Wiethoff S, Hamada M, Rothwell JC. Variability in response to transcranial direct current stimulation of the motor cortex. Brain Stimul 2014;7:468–75.

[12] Elsner B, Kugler J, Pohl M, Mehrholz J. Transcranial direct current stimulation for improving spasticity after stroke: a systematic review with meta-analysis. J Rehabil Med 2016;48:565–70.

[13] Evans C, Bachmann C, Lee J, Gregoriou E, Ward N, Bestmann S. Dose-controlled tDCS reduces electric field intensity variability at a cortical target site. Brain Stimul 2020.

[14] Laakso I, Tanaka S, Koyama S, De Santis V, Hirata A. Inter-subject Variability in Electric Fields of Motor Cortical tDCS. Brain Stimul Basic, Transl Clin Res Neuromodulation 2015;8:906–13. https://doi.org/10.1016/j.brs.2015.05.002.

[15] Minjoli S, Saturnino GB, Blicher JU, Stagg CJ, Siebner HR, Antunes A, et al. The impact of large structural brain changes in chronic stroke patients on the electric field caused by transcranial brain stimulation. NeuroImage Clin 2017;15:106–17.

[16] McCann H, Pisano G, Beltrachini L. Variation in Reported Human Head Tissue Electrical Conductivity Values. Brain Topogr 2019;32:825–58. https://doi.org/10.1007/s10548-019-00710-2.

[17] Huang Y, Datta A, Bikson M, Parra LC. Realistic vOlumetric-Approach to Simulate Transcranial Electric Stimulation -- ROAST -- a fully automated open-source pipeline. BioRxiv 2017. https://doi.org/10.1101/217331.

[18] Thielscher A, Antunes A, Saturnino GB. Field modeling for transcranial magnetic stimulation: a useful tool to understand the physiological effects of TMS? 2015 37th Annu. Int. Conf. IEEE Eng. Med. Biol. Soc., IEEE; 2015, p. 222–5.

[19] Dmochowski JP, Datta A, Bikson M, Su Y, Parra LC. Optimized multi-electrode stimulation increases focality and intensity at target. J Neural Eng 2011;8:46011.

[20] Huang Y, Thomas C, Datta A, Parra LC. Optimized tDCS for targeting multiple brain regions: an integrated implementation. 2018 40th Annu. Int. Conf. IEEE Eng. Med. Biol. Soc., IEEE; 2018, p. 3545–8.

[21] Dmochowski JP, Datta A, Huang Y, Richardson JD, Bikson M, Fridriksson J, et al. Targeted transcranial direct current stimulation for rehabilitation after stroke. Neuroimage 2013;75:12–9.

[22] Datta A, Baker JM, Bikson M, Fridriksson J. Individualized model predicts brain current flow during

transcranial direct-current stimulation treatment in responsive stroke patient. Brain Stimul Basic, Transl Clin Res Neuromodulation 2011;4:169–74.
[23] Galletta EE, Cancelli A, Cottone C, Simonelli I, Tecchio F, Bikson M, et al. Use of computational modeling to inform tDCS electrode montages for the promotion of language recovery in post-stroke aphasia. Brain Stimul Basic, Transl Clin Res Neuromodulation 2015;8:1108–15.
[24] Kim D-E, Park J-H, Schellingerhout D, Ryu W-S, Lee S-K, Jang MU, et al. Mapping the Supratentorial Cerebral Arterial Territories Using 1160 Large Artery Infarcts. JAMA Neurol 2019;76:72–80. https://doi.org/10.1001/jamaneurol.2018.2808.
[25] Hope TMH, Seghier ML, Leff AP, Price CJ. Predicting outcome and recovery after stroke with lesions extracted from MRI images. NeuroImage Clin 2013;2:424–33. https://doi.org/https://doi.org/10.1016/j.nicl.2013.03.005.
[26] Zhao L, Biesbroek JM, Shi L, Liu W, Kuijf HJ, Chu WW, et al. Strategic infarct location for post-stroke cognitive impairment: A multivariate lesion-symptom mapping study. J Cereb Blood Flow Metab 2018;38:1299–311. https://doi.org/10.1177/0271678X17728162.
[27] Huang Y, Datta A, Bikson M, Parra LC. Realistic vOlumetric-Approach to Simulate Transcranial Electric Stimulation--ROAST--a fully automated open-source pipeline. J Neural Eng 2019.
[28] Fang Q, Boas DA. Tetrahedral mesh generation from volumetric binary and grayscale images. 2009 IEEE Int. Symp. Biomed. Imaging From Nano to Macro, Ieee; 2009, p. 1142–5.
[29] Amadi U, Allman C, Johansen-Berg H, Stagg CJ. The Homeostatic Interaction Between Anodal Transcranial Direct Current Stimulation and Motor Learning in Humans is Related to GABAA Activity. Brain Stimul 2015;8:898–905. https://doi.org/10.1016/j.brs.2015.04.010.
[30] O'Shea J, Boudrias M-H, Stagg CJ, Bachtiar V, Kischka U, Blicher JU, et al. Predicting behavioural response to TDCS in chronic motor stroke. Neuro-Enhancement 2014;85, Part 3:924–33. https://doi.org/10.1016/j.neuroimage.2013.05.096.
[31] Fridriksson J, Richardson JD, Baker JM, Rorden C. Transcranial direct current stimulation improves naming reaction time in fluent aphasia: a double-blind, sham-controlled study. Stroke 2011;42:819–21.
[32] Baker JM, Rorden C, Fridriksson J. Using transcranial direct-current stimulation to treat stroke patients with aphasia. Stroke 2010;41:1229–36.
[33] Jenkinson M, Beckmann CF, Behrens TEJ, Woolrich MW, Smith SM. FSL. 20 YEARS FMRI 2012;62:782–90. https://doi.org/10.1016/j.neuroimage.2011.09.015.
[34] Laakso I, Mikkonen M, Koyama S, Ito D, Yamaguchi T, Hirata A, et al. Electric field dependent effects of motor cortical TDCS. BioRxiv 2018. https://doi.org/10.1101/327361.
[35] Bestmann S, Ward N. Are current flow models for transcranial electrical stimulation fit for purpose? Brain Stimul 2017;10:865–6. https://doi.org/10.1016/j.brs.2017.04.002.
[36] van Lier A, Kolk A, Brundel M, Hendriske J, Luijten J, Lagendijk J, et al. Electrical conductivity in ischemic stroke at 7.0 Tesla: a case study. Proc. 20th Sci. Meet. Int. Soc. Magn. Reson. Med., vol. 3484, 2012.
[37] Rekik I, Allassonnière S, Carpenter TK, Wardlaw JM. Medical image analysis methods in MR/CT-imaged acute-subacute ischemic stroke lesion: Segmentation, prediction and insights into dynamic evolution simulation models. A critical appraisal. NeuroImage Clin 2012;1:164–78.
[38] Tuch DS, Wedeen van J, Dale AM, George JS, Belliveau JW. Conductivity mapping of biological tissue using diffusion MRI. Ann N Y Acad Sci 1999;888:314–6.
[39] Tuch DS, Wedeen VJ, Dale AM, George JS, Belliveau JW. Conductivity tensor mapping of the human brain using diffusion tensor MRI. Proc Natl Acad Sci 2001;98:11697–701.
[40] Thiel CM, Zilles K, Fink GR. Cerebral correlates of alerting, orienting and reorienting of visuospatial attention: an event-related fMRI study. Neuroimage 2004;21. https://doi.org/10.1016/j.neuroimage.2003.08.044.
[41] van der Zijden JP, van der Toorn A, van der Marel K, Dijkhuizen RM. Longitudinal in vivo MRI of alterations in perilesional tissue after transient ischemic stroke in rats. Exp Neurol 2008;212:207–12.